Available online at www.sciencedirect.com
ScienceDirect
Catalysis Today 131 (2008) 444–449
CATALYSIS TODAY
www.elsevier.com/locate/cattod

Promotion effect of cerium and lanthanum oxides on Ni/SBA-15 catalyst for ammonia decomposition

Hongchao Liu [a,b], Hua Wang [a], Jianghan Shen [a,b], Ying Sun [a,b], Zhongmin Liu [a,*]

[a] *Applied Catalysis Laboratory, Dalian Institute of Chemical Physics, Chinese Academy of Sciences, 457 Zhongshan Road, Dalian 116023, Liaoning, PR China*
[b] *Graduate University of the Chinese Academy of Sciences, Beijing 100049, PR China*

Available online 26 November 2007

Abstract

CeNi/SBA-15 and LaNi/SBA-15 catalysts were prepared by deposition–precipitation (DP) method and characterized by N_2 physical adsorption, XRD, H_2-TPR, H_2-chemisorption and TEM. Their catalytic performances in the ammonia decomposition reaction were tested and compared with Ni/SBA-15 catalyst. Addition of cerium and lanthanum oxides to the Ni/SBA-15 catalyst caused some decrease of BET surface area and pore volume of the catalysts, but led to a promotion effect to their catalytic activity which was closely related to the ratio of Ce (La)/Ni. The highest conversion of ammonia could be obtained when the Ce (La)/Ni ratio was around 0.3. The promotion effect is more evident on CeNi/SBA-15(0.3) than on LaNi/SBA-15(0.3) catalyst under identical reaction conditions. The CeNi/SBA-15 and LaNi/SBA-15 catalysts show smaller nickel particle size and easier reducibility in comparison with the Ni/SBA-15 catalysts.

Keywords: Ammonia decomposition; Ni/SBA-15 catalysts; Cerium; Lanthanum

1. Introduction

Ammonia decomposition has attracted much attention recently because it can produce CO_x-free hydrogen that is desirable for direct use as fuel of proton membrane fuel cell [1,2]. Moreover, ammonia can be readily stored and transported, which is beneficial for on-site hydrogen production [3,4].

Many types of metal-supported catalysts, such as Ru, Ir, Fe, and Ni-based catalysts, have been employed as catalysts in ammonia decomposition for the production of CO_x-free hydrogen [5–13]. Among these catalysts, Ru-based catalysts show the highest activity, but the high price renders their industrial application quite questionable. The development of non-precious metal catalysts is of much interest from industry and academia. Supported nickel catalysts, which are cheap and show high activity in hydrogenation and dehydrogenation reactions, are often used in a number of industrial processes, and have been proved to be active in ammonia decomposition [9–11].

The effect of La_2O_3 as a promoter in the ammonia decomposition reaction on catalytic performance has been reported for a series of Ni/Al_2O_3 catalysts [11,12]. A beneficial influence was observed on improving catalytic performance of Ni/Al_2O_3 catalysts with an appropriate addition of lanthanum oxides, which has been attributed to an enhancement of the intrinsic activity of each active site. Li et al. [13] investigated the effect of KOH as a promoter on the performance of Ru and Ni-supported catalysts in the ammonia decomposition reaction, respectively. They found that the improved effect of Ni-based catalysts was less evident than that of Ru-based catalysts which suggested that the influence of promoters was dependent on both active components and supports. In our recent study, a series of Ni/SBA-15 catalysts with narrow particles distribution and nano-sized nickel (2–7 nm) have been prepared by deposition–precipitation (DP) method and show better performance in ammonia decomposition [14]. For better understanding the structure sensitivity over the Ni-based catalysts which have been discussed in the literature [11–13,15], it is deserved to investigate the effect of promoters on the performance of Ni/SBA-15 catalysts prepared by the DP method on ammonia decomposition.

* Corresponding author. Tel.: +86 411 84685510; fax: +86 411 84685510.
E-mail address: liuzm@dicp.ac.cn (Z. Liu).

0920-5861/$ – see front matter © 2007 Elsevier B.V. All rights reserved.
doi:10.1016/j.cattod.2007.10.048

In this study, the Ni/SBA-15 catalysts modified by cerium and lanthanum, respectively, were prepared and characterized with N_2 physical adsorption, XRD, H_2-TPR, H_2-chemisorption and TEM. The influence of cerium (or lanthanum) as promoters on performance of the Ni/SBA-15 catalysts was investigated in detail.

2. Experimental

2.1. Catalyst preparation

The NiO/SBA-15 catalysts were prepared by the DP method which have been described previously [14]. 0.14 mol of Ni $(NO_3)_2{\cdot}6H_2O$ and 0.02 mol of nitric acid were dissolved in 300 ml of deionized water. Then 250 ml of this solution was added to freshly calcinated SBA-15 (1.95 g, supplied by Jilin University) and subsequently heated to 328 K in a thermostat vessel. The other 50 ml solution was used to dissolve 0.32 mol of urea and then mixed with the suspension. The mixture was stirred and heated at 363 K for 3 h. After drying, the sample was calcinated at 873 K for 3 h and then crushed into the particles of 40–60 mesh.

CeNi/SBA-15(x) and LaNi/SBA-15(x) (x represents Ce (or La)/Ni ratio) catalysts were prepared with impregnating NiO/SBA-15 (40–60 mesh) in an aqueous cerium and lanthanum nitrate solution ($Ce(NO_3)_3$ and $La(NO_3)_3$, respectively). After drying at room temperature, the samples were calcinated at 823 K for 3 h.

2.2. Catalyst characterization

The compositions of catalysts were measured on a Philips Magix X spectrometer. Powder XRD measurements were conducted on a D/max-rb type X-ray diffractometer using monochromatic Cu Kα radiation (λ = 1.5418). Specific surface area, pore size and pore volume of support and catalyst were calculated with the adsorption isotherm data measured on a NOVA-4000 physical adsorption series using liquid nitrogen as adsorbate at 77 K. Prior to measurement, the samples were degassed in vacuum at 573 K for 4 h to remove physically adsorbed components. A JEOL JEM2000EX electron microscope device was employed (at 120 kV) to obtain the morphology and particle size of the catalysts. H_2-TPR and H_2 pulse chemisorption measurements were conducted on an AutoChem 2910 chemisorption analyzer (Micromeritics) as described previously [14].

2.3. Catalytic test

The ammonia decomposition reaction was performed in a continuous flow fixed-bed quartz reactor (inner diameter: 6 mm) under the flow of pure NH_3 (flow rate: 50 ml/min) at atmospheric pressure. Prior to the reaction, the catalysts (0.1 g, 40–60 mesh) were reduced in situ with 25% H_2/He flow at 773 K for 5 h, and then flushed with He for 30 min. Analysis of the effluent was performed with an on-line Varian CP-3800 gas chromatograph equipped with a Poropak N column and a thermal conductivity detector.

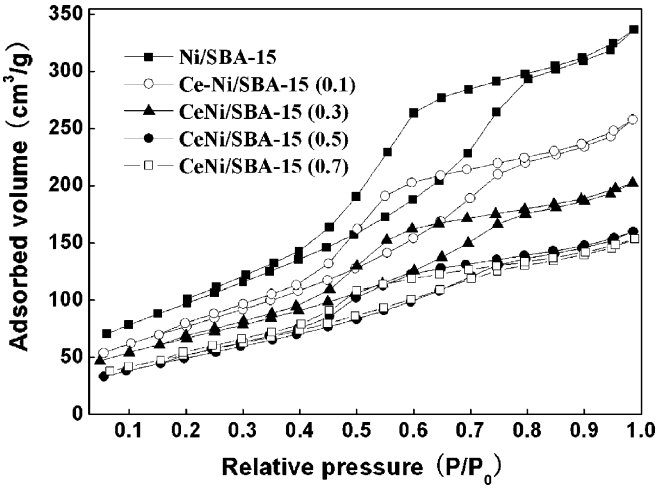

Fig. 1. Nitrogen adsorption and desorption isotherms of CeNi/SBA-15 catalysts.

3. Results and discussion

3.1. Textural properties of catalysts

3.1.1. BET surface area and pore structure

Figs. 1 and 2 exhibit the nitrogen adsorption–desorption isotherms of CeNi/SBA-15 and LaNi/SBA-15 catalysts. All the catalysts show type IV hysteresis loop isotherms, indicating that the mesoporous texture could be largely maintained although nickel and cerium or lanthanum was loaded successively on the SBA-15. But a loss in pore volume could be observed with the increasing of loading of cerium or lanthanum.

Table 1 depicts the physical properties of support and catalysts. It is obvious that the addition of cerium or lanthanum oxides reduces the surface area and pore volume of catalysts. Both the surface area and pore volume decrease whereas the

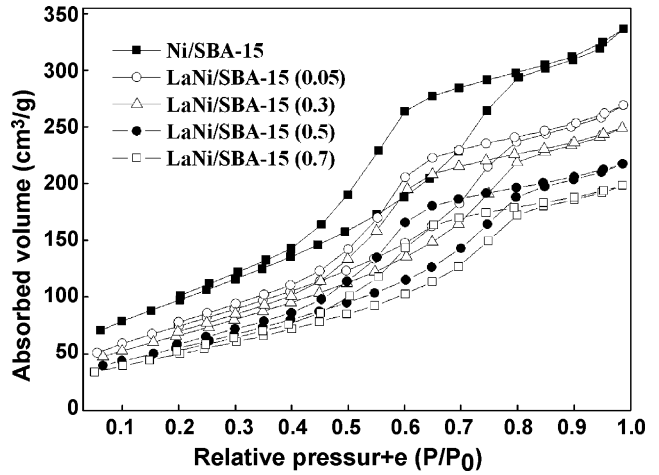

Fig. 2. Nitrogen adsorption and desorption isotherms of LaNi/SBA-15 catalysts.

Table 1
The physical properties of support and catalysts

Catalyst	S_{BET} (m^2/g)	V_P (ml/g)	D_P (nm)
SBA-15	839	1.26	6.59
Ni/SBA-15	365	0.55	4.31
LaNi/SBA-15(0.05)	285	0.45	4.90
LaNi/SBA-15(0.3)	254	0.42	4.91
LaNi/SBA-15(0.5)	213	0.37	4.89
LaNi/SBA-15(0.7)	189	0.36	4.91
CeNi/SBA-15(0.1)	290	0.43	3.82
CeNi/SBA-15(0.3)	246	0.33	3.82
CeNi/SBA-15(0.5)	191	0.27	3.82
CeNi/SBA-15(0.7)	199	0.25	3.82

pore size hardly changes with the increasing of Ce (La)/Ni ratio, indicating that most of the cerium or lanthanum oxides have entered into the pore systems, but no blockage of the pores occurs. Though the reduction has been observed with addition of the cerium and lanthanum, surface area higher than 180 m^2/g could be maintained for all catalysts.

3.1.2. TEM

Fig. 3 gives the TEM images of the catalysts reduced at 773 K for 5 h. Typical mesoporous structure of SBA-15 has been well-preserved for all the catalysts, in line with the nitrogen adsorption and desorption isotherms (Figs. 1 and 2). Narrow particles distribution and nano nickel particles lower than 5 nm could be observed for Ni/SBA-15 catalysts even for the catalysts with high loading of nickel (Fig. 3(a)). With regard to CeNi/SBA-15(0.3) and LaNi/SBA-15(0.3) catalysts, the larger particles in the TEM images appear due to the introduction of cerium oxides or lanthanum oxides (Fig. 3(b and c)), which could be assigned to cerium oxides and lanthanum oxides. Aside from the large particles of cerium or lanthanum oxides, narrow nickel distribution and nano nickel particles could be found for the LaNi/SBA-15(0.3) and CeNi/SBA-15(0.3) catalysts in Fig. 3(b and c).

3.2. X-ray diffraction

Fig. 4 exhibits the small-angle XRD patterns of LaNi/SBA-15 catalysts calcinated at 823 K for 3 h. Though relative intensity attenuates with the increasing of La/Ni ratio, an intense main diffraction peak and two weak peaks which are assigned to {1 0 0}, {1 1 0}, {2 0 0} reflection, respectively, are evident, implying that ordered hexagonal mesostructures of all the catalysts have been well-retained. The similar results can be obtained for LaNi/SBA-15 catalysts after reduction.

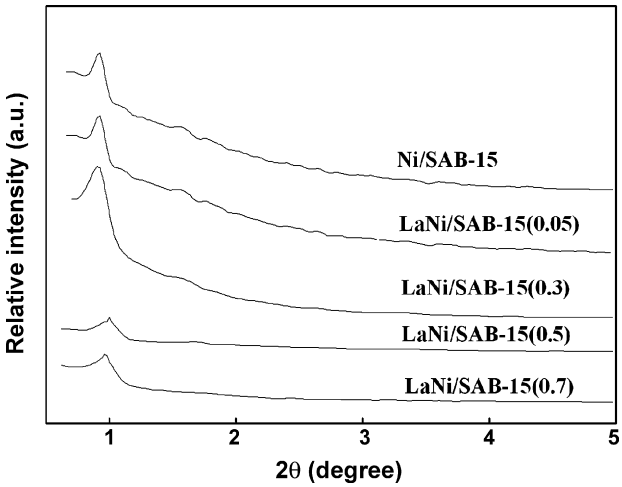

Fig. 4. Small-angle XRD patterns of Ni/SBA-15 catalysts promoted with lanthanum oxides after calcination at 823 K for 4 h.

Fig. 5 gives the wide-angle XRD patterns of LaNi/SBA-15 catalysts after calcination at 823 K for 3 h. It reveals that the characteristic peaks of NiO attenuate with the increasing of La/Ni ratio, indicating that La_2O_3 enhances the dispersion of NiO on support. This could be attributed to the interaction of NiO with La_2O_3 to form La–Ni mixed oxide or diluent effect aroused from the La addition causing separated small NiO particles which are too small to be detected [16,17]. The diffraction peaks of La_2O_3 are not present until the La/Ni ratio is above 0.5, suggesting that the La_2O_3 is high dispersed on the catalysts.

Fig. 6 shows the wide-angle XRD patterns of reduced LaNi/SBA-15 bodies. The peaks of NiO disappear after reduction at 773 K for 5 h, indicating that the NiO was completely reduced. On the other hand, the gradual intensity reduction of the peaks from Ni^0 and their disappearance with the increasing of lanthanum oxides, suggesting that the particle size decreases

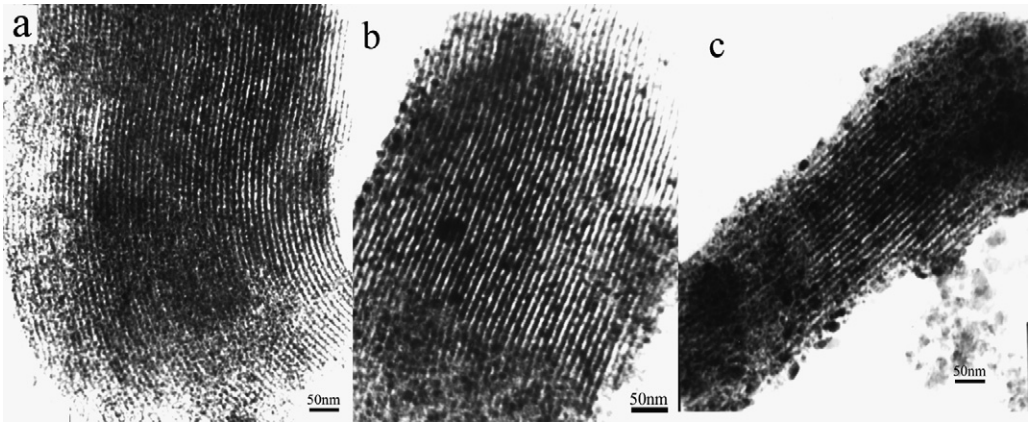

Fig. 3. TEM images of (a) Ni/SBA-15, (b) LaNi/SBA-15(0.3) and (c) CeNi/SBA-15(0.3) after reduction at 773 K for 5 h.

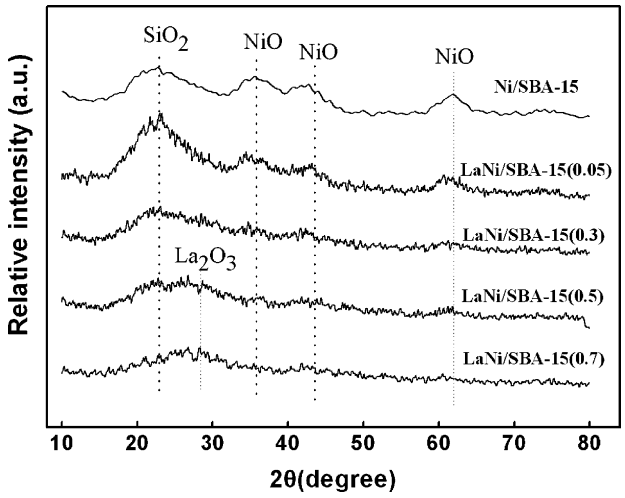

Fig. 5. Wide-angle XRD patterns of Ni/SBA-15 catalysts promoted with lanthanum oxides after calcination at 823 K for 4 h.

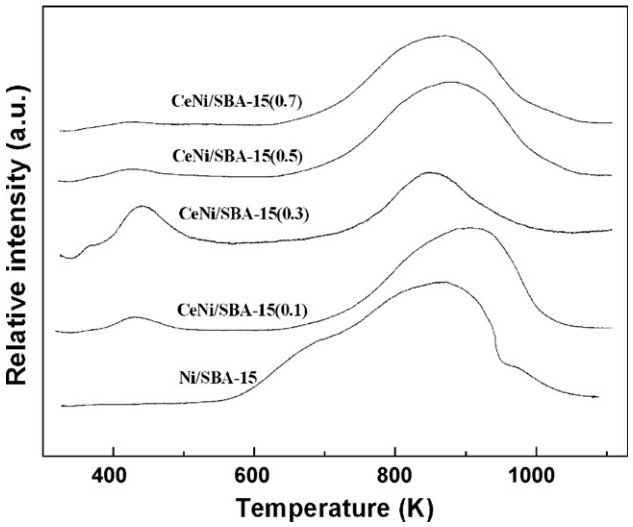

Fig. 7. TPR profiles of Ni/SBA-15 catalysts promoted with different loading of cerium.

with the modification of lanthanum. XRD patterns of the CeNi/SBA-15 catalysts are close to that of LaNi/SBA-15 catalysts. These results demonstrated that addition of cerium oxides or lanthanum oxides are beneficial for reducing particle size of Ni.

3.3. Promotion effect on catalyst reducibility and morphology

3.3.1. H_2- Temperature-program reduction (H_2-TPR)

Fig. 7 shows the H_2-TPR profiles of Ni/SBA-15 and CeNi/SBA-15 catalysts. The H_2-TPR profile of Ni/SBA-15 catalyst exhibits a broad asymmetric peak with a maximum at around 869 K and a shoulder peak at around 687 K, arising from the reduction of supported 1:1 nickel phyllosilicate [15,18,19]. The influence of the addition of cerium on reduction of nickel oxides is obvious. A weak peak around 430 K, corresponding to the reduction of black Ni_2O_3 [20,21], appears for all the Ce-promoted catalysts. The intensity of this peak is associated with the amount of Ni_2O_3 and is the highest when the Ce/Ni is around 0.3. However, the feature of Ni_2O_3 is not present in the XRD patterns (Fig. 5), indicating that Ni_2O_3 is highly dispersed for LaNi/SBA-15 catalysts. On the other hand, the broad peaks around 860 K, originating from the reduction of NiO, shift to lower temperature except the samples of Ce/Ni ratio around 0.1, and relative intensity of these peaks decreases with the increasing of La/Ni ratio. The occurrence of Ni_2O_3 and the shift of the broad peaks to lower temperature indicate that the less reducibility could be obtained due to the introduction of cerium on Ni/SBA-15 catalysts.

Fig. 8 displays the comparison of TPR profiles between Ni/SBA-15, LaNi/SBA-15(0.3) and CeNi/SBA-15(0.3). The peaks of both LaNi/SBA-15(0.3) and CeNi/SBA-15(0.3) appear at around 430 K, suggesting that the formation of Ni_2O_3 proceeds whether cerium or lanthanum oxides is added on Ni/SBA-15

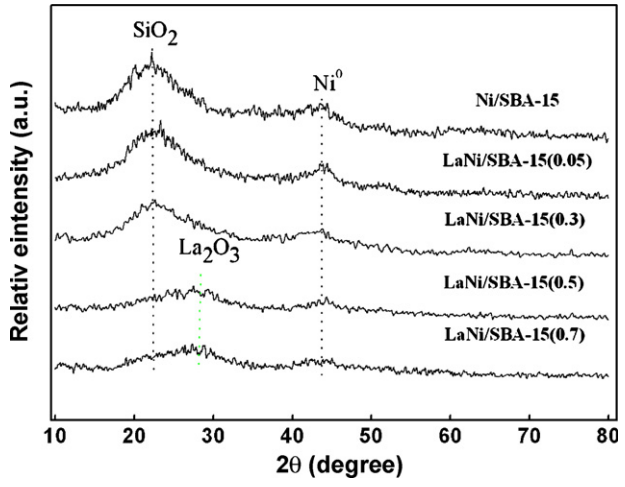

Fig. 6. Wide-angle XRD patterns of Ni/SBA-15 catalysts promoted with lanthanum oxides after reduction at 773 K for 5 h.

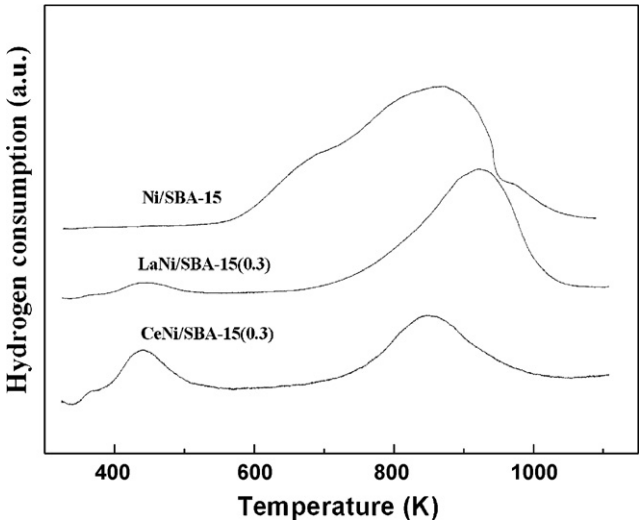

Fig. 8. TPR profiles of Ni/SBA-15 catalysts promoted with cerium and lanthanum oxides.

Table 2
H_2 chemisorption data on Ni/SBA-15 catalysts promoted with cerium and lanthanum after reduction under H_2 at 873 K for 1 h

Catalyst	Ni surface area, SA_{Ni} (m^2/g-cat)	Ni dispersion, D_{Ni} (%)	d_{Ni} (nm)
Ni/SBA-15	27.7	17.8	5.7
CeNi/SBA-15(0.3)	45.9	29.5	3.4
La Ni/SBA-15(0.3)	37.8	24.3	4.2

catalysts. The other peak above 800 K of LaNi/SBA-15(0.3) shifts to higher temperatures compared to that of Ni/SBA-15 whereas that of CeNi/SBA-15(0.3) is contrary. This indicated that the LaNi/SBA-15(0.3) catalyst is less reducible than Ce-Ni/SBA-15(0.3) catalyst. Natesakhawat et al. [22] also found that the CeNi/Al_2O_3 catalyst exhibited more evident promotion effect than the LaNi/Al_2O_3 catalyst in the investigation of effect of lanthanide oxides as sol–gel Ni/Al_2O_3 catalysts' promoters in steam reforming of propane. The results indicate that the presence of cerium oxides and lanthanum oxides would vary the reducibility of the catalysts which correlates with catalytic performance.

3.3.2. H_2 chemisorption

H_2 chemisorption experiments were performed to determine the nickel surface area and nickel dispersion of catalysts, and the results are listed in Table 2. The nickel dispersion and nickel surface area were calculated assuming that one hydrogen atom is adsorbed on one surface nickel atom, and the average nickel particle size was derived from the results of nickel dispersion of catalysts [23,24]. As listed in Table 2, high metal dispersion (17.8–29.5%) is observed for all catalysts. It also reveals that the addition of cerium or lanthanum reduces the nickel particle size. These are in agreement with the results of XRD patterns shown in Fig. 5. The nickel surface area and nickel dispersion of catalysts increase in the following order: Ni/SBA-15 < LaNi/SBA-15(0.3) < CeNi/SBA-15(0.3).

3.4. Promotion effect of addition of cerium and lanthanide oxides on catalytic performance

Fig. 9 presents the catalytic performance of Ni/SBA-15, CeNi/SBA-15 and LaNi/SBA-15 at various reaction temperatures. One can see that ammonia conversion over Ni/SBA-15 catalyst increases from 28.3% to 99.7% when the reaction temperature raises from 723 K to 923 K with $GHSV_{NH3}$ of 30,000 ml/g-cat h, and the Ni/SBA-15 catalysts shows higher activity than that prepared by impregnation methods under the identical reaction condition [14]. With regard to the effect of addition of cerium on the catalytic performance, we can see that ammonia conversion increases with the initial rises of cerium amount, and a maximum conversion (97% at 873 K) could be obtained when the Ce/Ni atomic ratio is around 0.3. However, further increase of the Ce/Ni atomic ratio will lead to a decrease of catalytic activity. The promotion effect of lanthanum on catalytic performance is similar to that of cerium depicted in Fig. 9. The results indicated that the appropriate addition of cerium and lanthanum as the promoters of Ni/SBA-15 catalysts would improve catalytic performance in ammonia decomposition. The optimal value of the Ce/Ni (or La/Ni) atomic ratio is around 0.3. Moreover, the promotion effect of cerium on catalytic performance is more evident than that of lanthanum.

Due to the introduction of cerium or lanthanum, a decrease in the BET surface area and pore volume could be observed. The catalytic performances were improved because of the reduction of nickel particle size. Previous study has proved that ammonia decomposition over the nickel catalysts is structure sensitive [11–14], so the changes of catalyst morphology should be one reasonable interpretation for the promotion effect of cerium or lanthanum. Moreover, lanthanides are known as strong-metal support oxides [25] and the interaction between nickel and cerium oxides would increase the nickel electron density accompanied by a crystal field effect [26]. Aika and coworkers [27–29] have reported a series of investigations on the effect of lanthanide oxide as a promoters or support on catalytic performance for ruthenium catalysts in ammonia

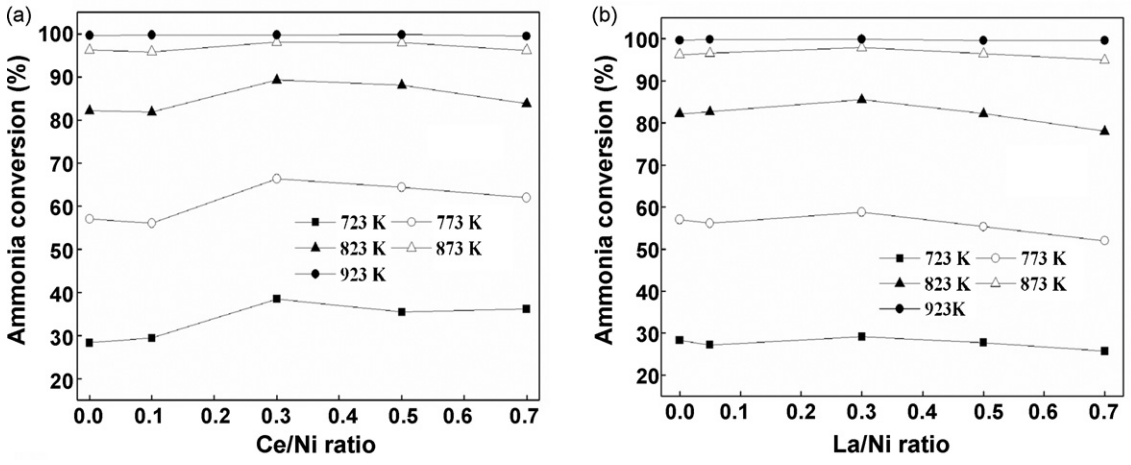

Fig. 9. Catalytic performance of (a) CeNi/SBA-15 and (b) LaNi/SBA-15 for ammonia decomposition at different reaction temperatures.

synthesis. They attributed the improved catalytic activity to the formation of low-valency lanthanide oxides partly on active metal surfaces after the catalyst was treated under hydrogen at high temperatures. More predominant improvement of catalytic performance could be observed in cerium oxides added Ni/SBA-15 than La_2O_3 modified catalyst. The reduced state of Ce_2O_3, which would cover the nickel surface to produce strong interaction between metal and promoter, is much stable than that of La_2O_{3-x} [28]. Thus, the electronic effect originated from the interaction between nickel and reduced the cerium oxide (lanthanum oxide) in ammonia decomposition is also possible although no direct evidences. Zhang et al. [12] also considered this as one reason for the enhanced performance of Ni/Al_2O_3 catalysts in ammonia decomposition. The decrease of catalytic activity with increase of the lanthanide amount should be attributed to that reduced accessible active components caused by the blockage of excess lanthanide oxides.

4. Conclusion

The appropriate additions of cerium and lanthanum to Ni/SBA-15 catalysts, which were prepared by the DP method, proved be effective in the ammonia decomposition reaction and the highest activity could be obtained when the Ce (La)/Ni ratio was around 0.3. The enhancement of catalytic activity with addition of cerium or lanthanum oxide stems from the enhancement of nickel surface area and nickel dispersion and changes of reducibility of catalysts. Morphological and electronical effects are very possibly responsible for the effective promotion on catalytic performance due to the addition of lanthanide oxide.

Reference

[1] T.V. Choudhary, C. Sivadinarayana, D.W. Goodman, Catal. Lett. 72 (3–4) (2001) 197.
[2] A.S. Chellappa, C.M. Fisher, W.J. Thomson, Appl. Catal. A 227 (2002) 231.
[3] R. Metkemeijer, P. Achard, Int. J. Hydrogen Energy 19 (1994) 535.
[4] R. Metkemeijer, P. Achard, J. Power Sources 49 (1994) 271.
[5] D. Szmigiel, W. Raróg-Pilecka, E. Miśkiewicz, Z. Kaszkur, Z. Kowalczyk, Appl. Catal. A 264 (2004) 59.
[6] S.F. Yin, Q.H. Zhang, B.Q. Xu, W.X. Zhu, C.F. Ng, C.T. Au, J. Catal. 224 (2004) 384.
[7] S.F. Yin, B.Q. Xu, S.J. Wang, C.F. Ng, C.T. Au, Catal. Lett. 96 (3–4) (2004) 113.
[8] S.F. Yin, B.Q. Xu, C.F. Ng, C.T. Au, Appl. Catal. B 48 (2004) 237.
[9] S.F. Yin, B.Q. Xu, S.J. Wang, C.T. Au, Appl. Catal. A 301 (2006) 202.
[10] J. Zhang, H.Y. Xu, Q.J. Ge, W.Z. Li, Catal. Commun. 7 (2006) 148.
[11] J. Zhang, H.Y. Xu, X.L. Jin, Q.J. Ge, W.Z. Li, Appl. Catal. A 290 (2005) 87.
[12] J. Zhang, H.Y. Xu, W.Z. Li, Appl. Catal. A 296 (2005) 257.
[13] X.K. Li, W.J. Ji, J. Zhao, S.J. Wang, C.T. Au, J. Catal. 236 (2005) 181.
[14] H.C. Liu, H. Wang, J.H. Shen, Y. Sun, Z.M. Liu, Appl. Catal. A revised.
[15] M. Grunze, M. Golze, R.K. Driscoll, P.A. Dowben, J. Vac. Sci. Technol. 18 (2) (1981) 611.
[16] J.S. Ledford, M. Houalla, A. Proctor, D.M. Hercules, J. Phys. Chem. 93 (1989) 6770.
[17] L.F. Zhang, J.F. Lin, Y. Chen, J. Chem. Soc. Faraday Trans. 88 (3) (1992) 497.
[18] P. Burattin, M. Che, C. Louis, J. Phys. Chem. B 101 (1997) 7060.
[19] P. Burattin, M. Che, C. Louis, J. Phys. Chem. B 104 (2000) 10482.
[20] B. Mile, D. Stirling, M.A. Zammitt, A. Lovell, M. Wwbb, J. Catal. 114 (1988) 217.
[21] B. Mile, D. Stirling, M.A. Zammitt, J. Mol. Catal. 62 (1990) 179.
[22] S. Natesakhawat, O. Oktar, U.S. Ozakan, J. Mol. Catal. A. 241 (2005) 133.
[23] C.H. Bartholomew, R.B. Pannell, J. Catal. 45 (1976) 41.
[24] C.H. Bartholomew, R.B. Pannell, J. Catal. 65 (1980) 390.
[25] S.J. Tauster, Acc. Chem. Res. 20 (1987) 389.
[26] E. Ramaroson, J.F. Tempere, M.F. Gullleux, J. Chem. Soc. Faraday Trans. 88 (8) (1992) 1211.
[27] S. Murata, K. Aika, J. Catal. 136 (1992) 118.
[28] Y. Niwa, K. Aika, J. Catal. 162 (1996) 138.
[29] Y. Kadowaki, K. Aika, J. Catal. 161 (1996) 178.